

# Shear mode AlN thin film electro-acoustic resonant sensor operation in viscous media

G. Wingqvist\*, J. Bjurström, L. Liljeholm, V. Yantchev, I. Katardjiev

*Department of Solid State Electronics, Box 534, Uppsala University, 751 21 Uppsala, Sweden*

Received 19 May 2006; received in revised form 13 September 2006; accepted 14 September 2006

Available online 2 November 2006

## Abstract

A shear mode thin film bulk acoustic resonator (FBAR) operating in liquid media together with a microfluidic transport system is presented. The resonator has been fabricated utilizing a recently developed reactive sputter-deposition process for AlN thin films with inclined *c*-axis relative to the surface normal with a mean tilt of around 30°. The resonator has a resonance frequency of around 1.2 GHz and a *Q* value in water of around 150. Sensor operation in water and glycerol solutions is characterized. Theoretical analysis of the sensor operation under viscous load as well as of the sensitivity and stability in general is presented. The theoretical predictions are compared with experimental measurements. The results demonstrate clearly the potential of FBAR biosensors for the fabrication of highly sensitive low cost biosensors, bioanalytical tools as well as for liquid sensing in general.

© 2006 Elsevier B.V. All rights reserved.

**Keywords:** Thickness mode resonator; Quasi-shear polarized acoustic wave; FBAR; AlN; Tilted films; Biosensor

## 1. Introduction

In recent years, the thin film electro-acoustic technology has made substantial progress particularly in view of high frequency Thin film bulk acoustic resonators (FBAR) for filters in telecom applications. The driving force behind the development of the thin-film technology has been the need to replace the use of expensive single crystalline substrates in the lower GHz region with piezoelectric thin film materials which would provide a wider choice of substrate materials and the prospect of mass production of low cost components integrated with the associated electronics. Reactive sputtering is a commonly used method for the deposition of thin films, since it is compatible with the planar technology in addition to being a low temperature technique with excellent thickness uniformity. A number of attempts to utilize FBAR devices for different sensor applications, including both gaseous and liquid phase sensing, have been reported in the last decade [1,2]. They report of limited success for in-liquid operation since they have been restricted to the longitudinal mode of operation which results in acoustic energy being radiated out

into the liquid through compressional motion. The shear polarization has proven to be the preferred choice for liquid operation of bulk acoustic resonators as well as of plate mode and surface acoustic resonators. Shear acoustic waves do not produce any compressional motion into the liquid and thereby no energy leakage [3]. Quite recently, it was reported of a low temperature reactive sputter deposition process for AlN films with a 30° tilt of the *c*-axis, which does not require any additional hardware modification and is completely independent of the properties of the substrate as well as is characterized with an excellent tilt uniformity [4]. It has also been demonstrated experimentally that the inclined AlN thin films grown with the latter process are suitable for the fabrication of shear mode TFBARs for liquid phase mass sensors such as biosensors and that mass loading from different concentrations of albumin could be resolved [5].

One of the most successful examples of electro-acoustic liquid phase sensors has been the commonly used quartz crystal microbalance (QCM) [6]. There are, however, a number of significant differences between the QCM and the FBAR sensors as follows.

First of all, the frequency of operation of FBARs is typically about 200 times higher than that of QCM. Most generally, this leads to a much higher mass sensitivity, as the latter is a square function of the frequency. Another frequency dependent

\* Corresponding author.

E-mail address: [gunilla.wingqvist@angstrom.uu.se](mailto:gunilla.wingqvist@angstrom.uu.se) (G. Wingqvist).

effect is the acoustic wave attenuation, normally considered as an absorption process due to material viscosity. For most of the materials the acoustic wave attenuation increases with the square of frequency leading to a quality factor degradation directly proportional to the frequency of operation. Thus, the beneficial effect of the increased sensitivity on the resolution at high frequencies is moderated by the increased device instability [7]. In other words, these frequency dependencies have a significant impact on the overall sensor resolution [7] and a trade-off is to be pursued.

Secondly, FBARs are generally made of polycrystalline materials, which introduce some uncertainties in the materials properties.

Thirdly, because of the significantly higher frequency of operation FBARs are much more thinner than QCM making them more fragile and susceptible to external loadings. Further, the thickness of the piezo-material becomes comparable with that of the electrodes, which in turn makes the FBAR heavily loaded with a non-piezoelectric material, thus presuming a significant impact of the electrode material and thickness over the sensor performance. Hence, the latter will lead to substantial deviations in the frequency shift due to viscosity variations (see below) from the Stockbridge–Kanazawa theory [8,9]. A more precise theoretical treatment, based on the Nowotny–Benes model [10], including the influence of the electromechanical coupling as well as that of the electrodes and the acoustic wave polarization angle is provided inhere. In this analysis the damping due to viscous loads is specifically addressed since its understanding will allow FBAR design optimization for in-liquid operation in view of improved sensitivity-to-noise ratio. The theoretical calculations are compared with experiment.

## 2. Experimental

### 2.1. Fabrication

Standard FBAR structures with a tilted AlN film were fabricated on 4 in. Si wafers using the reactive sputtering process presented in [4]. The bottom (and eventually the top) 200 nm thick Al electrodes were patterned with standard lithography and dry etching processes. Next, a 2  $\mu\text{m}$  thick AlN film was deposited and subsequently patterned to open contact holes to the bottom electrode from the top side. The overlap between the top and bottom electrode defines the active area of  $300\ \mu\text{m} \times 300\ \mu\text{m}$  within which the acoustic wave is excited. The top electrode has an asymmetric geometry to suppress the lateral excited modes [11]. Figs. 1 and 2 show a schematic of the resonator

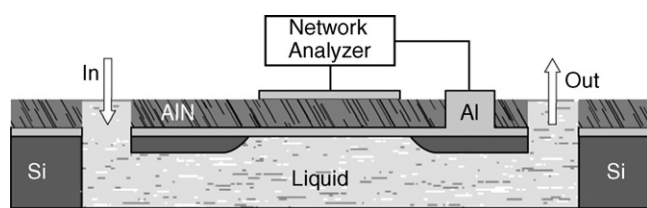


Fig. 1. Schematic illustration of a shear mode FBAR resonator together with a microfluidic transport system.

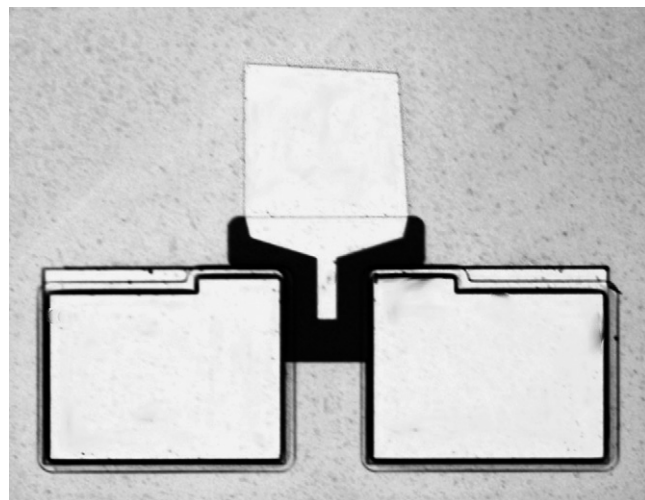


Fig. 2. Top view of the resonator. The ground contact pads are connected via contact holes to the bottom electrode, while the signal contact pad in the middle is connected to the top electrode.

in cross-section as well as top view of the fabricated resonator respectively. Finally, the silicon wafers are etched from the backside, thus defining the freestanding thin film membrane. This is done both to isolate the resonator acoustically from the substrate as well as to create a cavity underneath the resonator containing the liquid to be analyzed. The cavity is further connected to the top Si surface through a series of horizontal and vertical channels, which form the microfluidic transport system for analyte delivery to the bottom electrode of the resonator, see Fig. 3.

### 2.2. Electrical characterization

One port electrical characterisation was performed with a HP 8720D network analyzer by measuring the resonator admit-



Fig. 3. Photographic image of the measurement set-up. The probing to the contacts is performed with a pico-probe seen at the bottom of the photograph. The inlet and outlet pipes seen on either side of the pico-probe are connected to the microfluidic channel system of the resonator via an o-ring seal.

tance as a function of frequency. The instrument is limited to 1601 measurements points within a frequency sweep. In order to improve the resolution for determining the resonance frequency mathematical curve fits to both the admittance and the impedance were made subsequently, from which fits the series and parallel resonance frequencies are derived respectively. Similarly, the series and parallel loaded  $Q$  values are calculated directly from the slope of the phase as

$$Q = \frac{f_0}{2} \left. \frac{\partial \Phi}{\partial f} \right|_{f_0}, \quad (1)$$

where the  $f_0$  is the series and parallel resonance frequency and  $\Phi$  is the phase of the impedance.

The dissipation  $D$  is generally defined as  $1/Q$ . The total dissipation  $D_{\text{tot}}$  is the summation of the device dissipation in air  $D_0$  and the dissipation due to the viscous load  $D_{\text{visc\_load}}$  as

$$D_{\text{tot}} = D_0 + D_{\text{visc\_load}} = \frac{1}{Q_0} + \frac{1}{Q_{\text{visc\_load}}} = \frac{1}{Q_{\text{tot}}}. \quad (2)$$

The  $D_{\text{visc\_load}}$  is then derived as  $D_{\text{tot}} - D_0$ .

### 3. Results and discussion

To avoid tedious repetition in the presentation it is noted that unless stated otherwise all experiments and calculations are done for shear mode AlN FBAR sensors having one of the surfaces in contact with a liquid while the other surface being in contact with air. The materials constants of single crystalline AlN are used in the calculations.

#### 3.1. Performance of the resonator

The resonance frequency of the shear mode was typically, in the range 1.2–1.6 GHz depending on the film and electrode thickness, the electromechanical coupling around 2% and the quality factor about 350 when operated in air. To create a biochemically suitable surface for the subsequent experiments a 20 nm thick Au layer was thermally evaporated onto the backside of the wafer. The latter resulted in a 50 MHz decrease of the resonance frequency as well as in a reduction of both the quality factor and the electromechanical coupling. A typical resonator response in air is shown in Fig. 4, where both the quasi-longitudinal and the quasi-shear modes are clearly seen.

The resonator was then characterized in pure water. Fig. 5 illustrates the influence of water on the impedance response of both the shear and the longitudinal mode for the resonator presented in Fig. 4 above. As seen, the response of the shear mode is damped to a limited extent, while that of the longitudinal mode has considerably deteriorated. The  $Q$ -values of the shear mode FBAR are 310 (in air) and 150 (in water), respectively while those of longitudinal FBAR are 220 (in air) and 30 (water), respectively. In view of Eq. (2), this means that the dissipation in water  $D_{\text{visc\_load}}$  is 0.0034 and 0.029 for the shear and longitudinal mode, respectively.

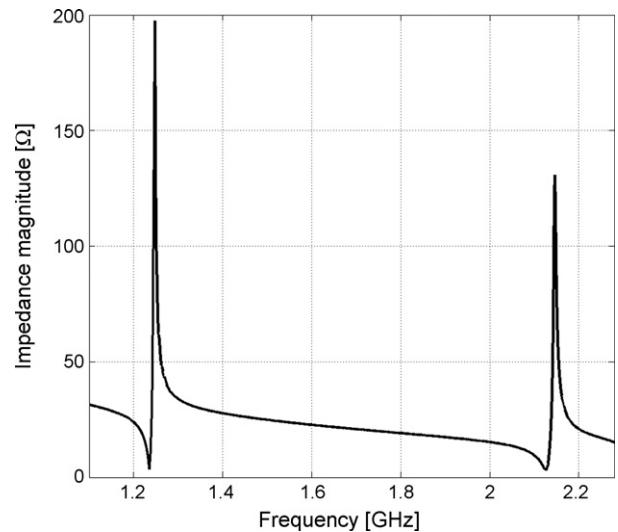


Fig. 4. Impedance magnitude vs. frequency for an AlN shear mode FBAR operated in air. Clearly seen are the resonances of the shear mode at 1.25 GHz and the longitudinal mode at 2.15 GHz.

#### 3.2. Effects of the polarization angle and the electromechanical coupling

A variety of factors can affect the optimal performance of a resonator sensor in viscous media. We now examine those ones stemming from effects related to the polarization angle and the electromechanical coupling. The polarization angle here is defined as the deviation of the polarization vector from that in the isotropic case, where only pure shear and longitudinal modes exist. These effects were studied theoretically and illustrated experimentally. In the first instance, a resonator consisting solely of a piezoelectric AlN film was considered (bare FBAR) to exclude the influence of the electrodes. In hexagonal AlN films with inclined  $c$ -axis two thickness excited modes can be observed—one quasi-longitudinal and one quasi-shear. These are not pure modes since the polarization angle is not zero. Such

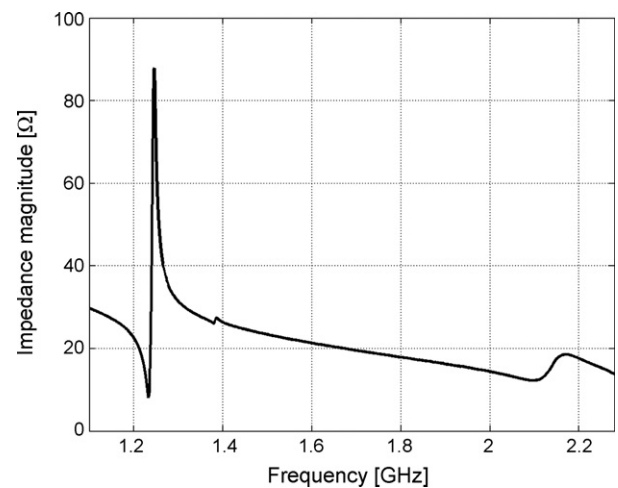


Fig. 5. Impedance magnitude vs. frequency for an AlN shear mode FBAR operated with one side in contact with water. Clearly seen are the resonances of the shear mode at 1.25 GHz and the almost totally damped longitudinal mode at 2.15 GHz.

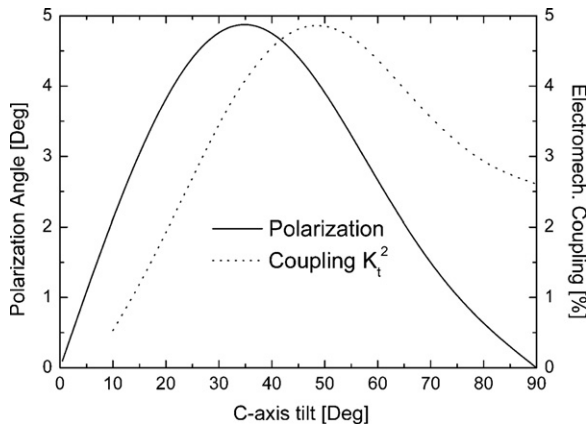


Fig. 6. Polarization angle (solid line) and the electromechanical coupling  $k_t^2$  (dotted line) for the quasi-shear mode with varying tilt of the crystallographic  $c$ -axis of AlN.

a deviation gives rise to a degeneration of the wave when propagating in an isotropic liquid. [12,13] Thus, one pure-shear and one pure-longitudinal degenerate modes originating from the original quasi-shear one, are formed at the solid/liquid interface. The longitudinal mode, being compressional, propagates accordingly into the liquid, thus dissipating its portion of the energy. The shear mode localizes its energy close to the surface, thus contributing to a slight shift in the resonance cavity. The shear mode, however, is reflected back into the solid with high efficiency, thus retaining its portion of the energy within the resonator. The impact of this degeneration effect on the FBAR performance is strongly dependent on the polarization angle of the shear mode as the latter determines the relative energy carried by the two degenerate modes. The polarization angle and the corresponding electromechanical coupling ( $k_t^2$ ) as a function of the  $c$ -axis tilt, shown in Fig. 6, are readily derived by solving the eigenvalue–eigenvector problem for the Christoffel set of equations [13]. Polarization angles not exceeding  $5^\circ$  are observed reaching a maximum value at  $35^\circ$   $c$ -axis tilt. Maximum electromechanical coupling of around 4.8% is achieved at  $47^\circ$   $c$ -axis tilt. For quantitative estimation of the impact of the polarization angle and coupling, the dissipation due to viscous losses  $D_{\text{visc.load}}$  is calculated with the Nowotny–Benes model as a function of the  $c$ -axis tilt for both low (pure water) and high (75% glycerol) viscous loads, respectively. These results are presented in Fig. 7. The simulations assume a bare piezoelectric AlN thickness excited shear resonator of a thickness of  $2\ \mu\text{m}$  and an area of  $300\ \mu\text{m} \times 300\ \mu\text{m}$  in contact with viscous media.

The results can easily be explained in terms of the Butterworth and Van Dyke (BVD) equivalent lumped circuit model (Fig. 8) which provides a direct relation between the measured electrical quantities and the physical properties of the resonant system [7]. Electrically, the system is represented by two parallel arms representing the static capacitance  $C_0$  of the structure and the acoustic wave contribution, respectively. The latter is typically called “motional arm” and is in a direct relation with the electro-acoustic properties of the materials used. At resonance, the motional capacitance  $C_m$  and the motional inductance

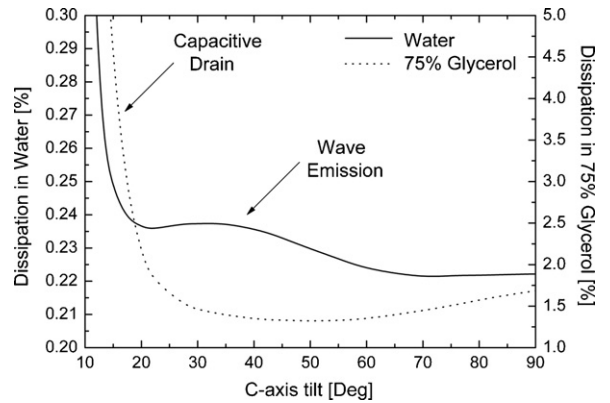


Fig. 7. The dissipation due to viscous load of the shear mode resonator operated in pure water (solid line) and in glycerol–water solution of 75% glycerol (dotted line) as a function of the  $c$ -axis tilt of AlN.

$L_m$  cancel each other and the resistance of the arm equals the motional resistance  $R_m$ . Thus, the behaviour of the resonator at resonance frequency is determined by the impedances of the static capacitance:

$$|Z_0| = \frac{1}{\omega C_0}, \tag{3}$$

as well as that of the motional resistance:

$$R_m = \frac{(\pi/2)^2 \alpha}{k_t^2 \omega C_0}. \tag{4}$$

Here  $\omega$  is the angular frequency,  $\alpha$  the acoustic wave attenuation and  $k_t^2$  the electromechanical coupling.

In the case of relatively low viscous loads (water) the dissipation exhibits two characteristic regions of increased dissipation (see Fig. 7). The first one, observed at small  $c$ -axis tilts and marked as “capacitive drain”, is related to the diminishing electromechanical coupling resulting in a substantially increased

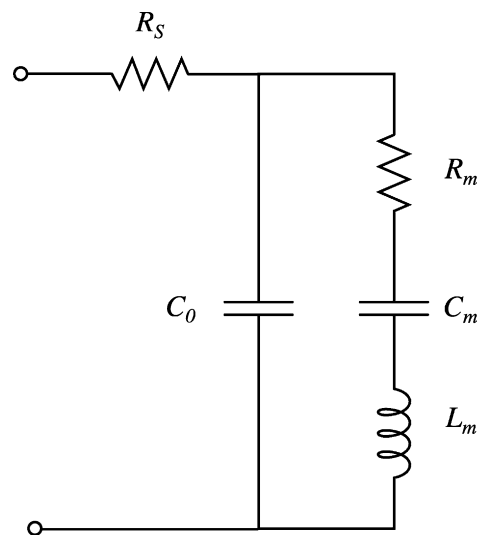


Fig. 8. The equivalent circuit of the Butterworth and Van Dyke model of a thickness excited resonator, where  $C_0$  is the clamped capacitance,  $R_s$  the series resistance and  $L_m$ ,  $C_m$  and  $R_m$  are the motional impedance, capacitance and resistance, respectively.

motional resistance, thus promoting significant device degradation due to electrical drain through the static capacitance. It is recalled that the motional resistance is proportional to the ratio between the overall losses and the electromechanical coupling (Eq. (4)). The second characteristic region, marked as “wave generation” appears at relatively high couplings and is related to the observed maximum in the polarization angle of the quasi-shear mode.

In other words, as the polarization angle increases the acoustic energy leakage through the degenerate longitudinal mode increases correspondingly as the energy carried by that mode increases accordingly. In the relatively large viscosity case the large viscous load generally results in an increased motional resistance (see Eq. (4)), which increase can only be compensated by high electromechanical coupling. Hence, the minimum in the dissipation observed in this case (Fig. 7) corresponds to the region of high couplings in Fig. 6. It is noted that the “wave generation” loss mechanism is still present in this case, but its magnitude is negligibly smaller than that of the viscous losses and hence, its contribution is marginal in comparison. Finally, the slight increase in the dissipation at high  $c$ -axis tilt angles is due to the decline in coupling which in this case is insufficient to compensate the large viscous losses.

The above findings can be summarized as follows. For viscous media with viscosity similar to that of water acoustic leakage through the degenerate longitudinal mode is appreciable for polarization angles larger than  $3^\circ$ . Optimal operation is achieved for  $c$ -axis tilts close to  $90^\circ$  (a-textured AlN films) where the mode is almost pure and the coupling is still sufficiently large to compensate for the viscous losses. For media with viscosity much larger than that of water the acoustic leakage losses can be neglected. Much more important in this case is the magnitude of the coupling coefficient, since high couplings counter weigh the large viscous losses yielding moderate values of the motional resistance (Eq. (3)). In both cases very low coupling coefficients yield very high motional resistance leading to deterioration of device operation through capacitive leakage. In such cases the only remedy is to tune out the static capacitance by additional circuitry [14]. Most generally it can be said that the deficiency in coupling increases with the viscosity. Needless to say that the above conclusions are strictly valid for the case of AlN although, qualitatively they can be extrapolated to arbitrary materials.

### 3.3. Effects of the viscosity of the surrounding media

Both the damping and the resonance frequency shift depend on both the viscosity and the density of the surrounding medium. A classical experiment for studying more or less exclusively the viscosity effects in QCM resonators has been their characterization at different concentrations of glycerol [15], since the glycerol density varies only marginally with the glycerol concentration. Here, we perform a similar characterization both theoretically and experimentally of FBARs by varying the glycerol concentration so that the viscosity was varied in the range 0.01 P (0% glycerol) to 0.20 P (70% glycerol). The simulations use the Nowotny–Benes model now assume a realistic resonator, corresponding to the one used for the experimental

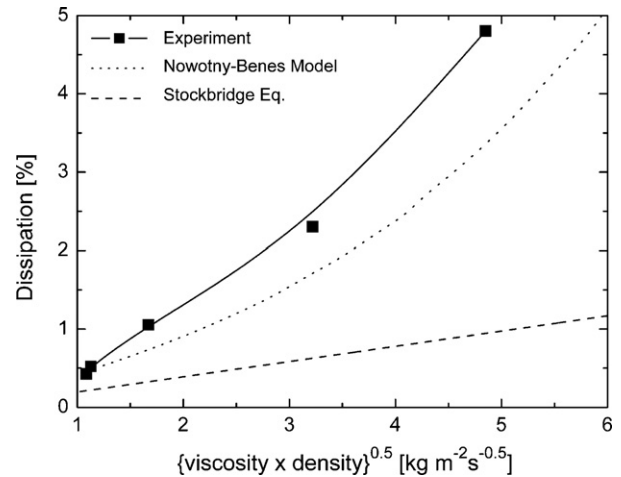


Fig. 9. The experimental results (squares), theoretical prediction using the Nowotny–Benes (dotted line) and theoretical predictions using the Stockbridge equation (dashed line) for the dissipation change of a FBAR in contact with liquid with varying viscosity.

measurements, consisting of 1750 nm thick AlN, 280 nm thick Al electrodes and 20 nm thick Au deposited on the side which is in contact with an infinite viscous medium. The tilt of the AlN film is assumed to be  $28^\circ$  while the area of the resonator is  $300 \mu\text{m} \times 300 \mu\text{m}$ . In Figs. 9 and 10 along with Table 1, the dissipation and the sensitivity obtained with the Nowotny–Benes and the Stockbridge models are compared with experimental measurements. Simulations were also made excluding the non-piezoelectric metal layers to study the influence of the electrodes on the dissipation. In Table 1, it can be noted that the presence of the contacts leads to a significant increase in the dissipation, especially at high viscous load, and that the addition of the 20 nm Au layer further increased the dissipation bringing the simulation even closer to the experimental values. The latter is associated with the acoustic matching between the metal layers and water. The latter effect promotes higher viscous sensitivity as well. It is noted that viscous damping within the soft metal materials is not included in the calculations; only damping due

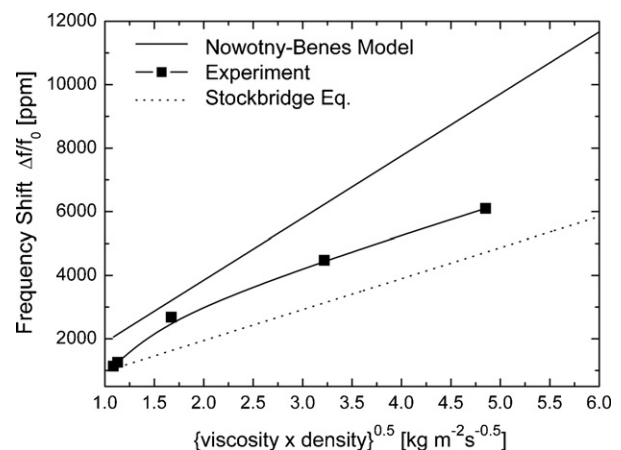


Fig. 10. Experimental results (squares), theoretical prediction using the Nowotny–Benes (dotted line) and theoretical predictions using the Stockbridge equation (dashed line) for the normalized frequency shift of a shear mode FBAR in contact with liquids of varying viscosity.

Table 1

Dissipation due to viscous load in water and in 70% glycerol calculated with Stockbridge equation and with the Nowotny–Benes method (NB) utilizing different resonator structures

	Stockbridge	NB without electrodes	NB with Al contacts	NB with Al contacts +20 nm Au	Experimental value
$\Delta D$ in water ( $\times 10^{-3}$ )	2.1	2.4	3.1	4.6	4.4
$\Delta D$ in 70% glycerol ( $\times 10^{-3}$ )	9.5	11	17	34	48

Corresponding experimental results are also presented.

to the viscous load from the liquid is taken into account. The one-dimensional treatment provided by the Nowotny–Benes model appears to be in a better agreement with the experimental observations, since it includes the effects of both capacitive drain and wave polarization in addition to taking into account the whole topology of the resonator. Expectedly, the dissipation and sensitivity predicted by the model are somewhat lower and higher, respectively as compared with the experiment. The observed differences can be attributed to two- and three-dimensional effects, not included in the analysis, related to the existence of a lateral component in the propagation vector. The latter is represented by the non-uniform distribution of the wave amplitude in the lateral direction promoting, thus an energy leakage through laterally propagating plate modes [16]. Typically these modes have a degrading influence over the device quality factor since they are uncoupled from the resonant cavity, thus being useless for sensing purposes. The Stockbridge model as seen deviates substantially from the experiment since it does not take into account the influence of the wave polarization and the electrical matching between the resonator static capacitance and its motional arm. It is to be noted that the influence of the electrical matching over the sensor performance is quite strong especially when high viscosities are to be measured.

#### 3.4. Mass sensitivity and resolution in viscous media

The resolution is defined by the ratio between the stability and sensitivity. Consequently estimations of the resolution requires estimation of the both the stability and sensitivity. In initial FBAR studies for sensor applications one major concern was the anticipated high noise level that would naturally result in insufficient resolution. It has recently been reported, however, that the mass resolution of shear mode FBAR sensors when operated in liquids is already of the same order as conventional QCM sensors [5,17]. To make a proper comparison, though, noise measurements and characterisation must be standardised. There exists an IEEE standard procedure suggesting how to calculate the noise of oscillators from data sets in the time domain commonly known as the Allan deviation [18]. In addition, a number of researchers use a different procedure known as the threefold standard deviation [17]. Table 2, shows one and the same stability measurement of a shear FBAR resonator represented in terms of both the Allan deviation and the threefold standard deviation, with its corresponding detection limit [5]. It is noted that these measurements were performed under non-controlled conditions, i.e. in an ordinary office environment without taking any precautions regarding temperature drift, humidity, vibrations, dust, etc. In the same context, it is

noted that the FBARs in this work normally exhibited a temperature coefficient of frequency in the range of  $-25$  ppm/ $^{\circ}$ C. As seen, a difference in the detection limit by up to a factor of 10 can be seen between the two methods. The point being made here is that reporting resolution figures in the literature is highly ambiguous unless the method for determining the stability is clearly specified.

As stated in the introduction FBARs represent heavily loaded resonators and as such the electrode properties are expected to have an appreciable impact on sensor performance, including sensor mass sensitivity. Estimation of the FBAR mass sensitivity was again done by employing both the NB model and the Sauerbrey equation. The mass sensitivity was calculated by adding a 0.2 nm gold layer onto two different structures operated at the same frequency. For a bare (without electrodes) 2500 nm thick AlN FBAR operating at 1.23 GHz the mass sensitivity in water is calculated to be  $1.5$  MHz  $\text{cm}^2/\mu\text{g}$  with the NB model and the same with the Sauerbrey equation. On the other hand, the mass sensitivity according to the NB model of a realistic FBAR structure for biosensor applications (1750 nm AlN, 280 nm Al bottom and top electrode and an additional 20 nm Au layer, for chemical stability) operating at the same frequency (1.23 GHz) is  $2.9$  MHz  $\text{cm}^2/\mu\text{g}$ , that is, almost a factor of 2 higher. The observed increase of mass sensitivity is attributed to the significant loading of the resonator. Since, the thickness of the electrodes in this case comprises almost one fourth of the total resonator thickness and the latter now represents a composite resonator. Under these conditions the first order approximation in the Taylor expansion of the mass sensitivity [19] is no longer valid and higher terms in the Taylor series have to be included, resulting in a non-linear behaviour of the mass sensitivity with mass loading. In addition, for proper estimation of the mass sensitivity of a composite resonator the material's constants of the electrodes need to be taken into consideration, which is the case with the NB model but not in the treatment in Ref. [19].

Finally using noise thresholds from both the Allan deviation and the threefold standard deviation as well as estimates of the

Table 2  
FBAR stability measurements in water under non-controlled conditions

	Series	Parallel
$Q$	160	140
$f$ (GHz)	1.236	1.245
Detection limit with Allan deviation (Hz)	856	298
Detection limit with standard deviation (Hz)	2922	3767

sensitivity based on both Sauerbrey and the NB model yields values for the resolution ranging from 0.3 ng/cm<sup>2</sup> to 7.5 ng/cm<sup>2</sup>, respectively.

#### 4. Conclusions

Thin film thickness excited shear acoustic wave resonant sensors have been designed, fabricated and characterized. The in-liquid performance of these devices has specially been addressed. The above results illustrate clearly that the tilted thin film electro-acoustic sensor technology represents a competitive alternative to the single crystal QCM technology, since it is characterized with extreme sensitivity, higher resolution, small size, low cost and is compatible with the standard IC technology. The mass resolution demonstrated even in a non-controlled environment excels that of QCM.

#### Acknowledgements

This work is supported by the Swedish Agency for Innovation Systems Foundation (Vinnova), the EU Biognosis project as well as by the Foundation for Strategic Research, Sweden through the ICTEA project. The technical support of Biosensor Applications AB is kindly acknowledged.

#### References

- [1] R. Brederlow, S. Zauner, A.L. Scholtz, K. Aufinger, W. Simburger, C. Paulus, A. Martin, M. Fritz, H.-J. Timme, H. Heiss, S. Marksteiner, L. Elbrecht, R. Aigner, R. Thewes, Biochemical sensors based on bulk acoustic wave resonators, in: IEEE International Electron Devices Meeting 2003, December 8–10, 2003, pp. 32.7.1–32.7.3.
- [2] H. Zhang, M.S. Marma, E.S. Kim, C.E. McKenna, M.E. Thompson, Implantable resonant mass sensor for liquid biochemical sensing, in: 17th IEEE International Conference on Micro Electro Mechanical Systems (MEMS): Maastricht MEMS 2004 Technical Digest, January 25–29, 2004, 2004, pp. 347–350.
- [3] D.S. Ballantine, R.M. White, S.J. Martin, A.J. Ricco, E.T. Zellers, G.C. Frye, H. Wohltjen, *Acoustic Wave Sensors; Theory, Design and Physico-chemical Applications*, Academic Press, 1997.
- [4] J. Bjurström, G. Wingqvist, I. Katardjiev, Synthesis of textured thin piezoelectric AlN films with a nonzero *c*-axis mean tilt, in: IEEE Ultrasonics Symposium Proceeding, vol. 1, 2005, pp. 321–324.
- [5] G. Wingqvist, J. Bjurström, L. Liljeholm, I. Katardjiev, A.L. Spetz, Shear mode AlN thin film electroacoustic resonator for biosensor applications, in: IEEE Sensor Proceedings, October 31, 2005, 2005, pp. 492–495.
- [6] R. Thalhammer, S. Braun, B. Devic-Kuhar, M. Groschl, F. Trampler, E. Benes, H. Nowotny, M. Kostal, Viscosity sensor utilizing a piezoelectric thickness shear sandwich resonator, IEEE Trans. Ultrason. Ferroelectr. Freq. Control 45 (1998) 1331–1339.
- [7] J.R. Vig, On acoustic sensor sensitivity, IEEE Trans. Ultrason. Ferroelectr. Freq. Control 38 (1991) 311.
- [8] C.D. Stockbridge, Effects of gas pressure on quartz-crystal microbalances, in: Presented at Fifth Conference on Vacuum Microbalance Techniques, 1965, Princeton, 1966.
- [9] K.K. Kanazawa, J.G. Gordon, Frequency of a quartz microbalance in contact with liquid 57 (1985) 1770–1771.
- [10] H. Nowotny, E. Benes, General one-dimensional treatment of the layered piezoelectric resonator with two electrodes, J. Acoust. Soc. Am. 82 (1987) 513–521.
- [11] I. Larson, D. John, R.C. Ruby, P. Bradley, Bulk acoustic wave resonator with improved lateral mode suppression, Agilent Technologies Inc., US, 2001.
- [12] N.F. Foster, G.A. Coquin, G.A. Rozgonyi, F.A. Vanatta, Cadmium sulphide and zinc oxide thin-film transducers, IEEE Trans. Sonics Ultrason. SU-15 (1968) 28–41.
- [13] J.F. Rosenbaum, *Bulk Acoustic Wave Theory and Devices*, Artech House, 1988.
- [14] I.D. Avramov, A 0-phase circuit for QCM-based measurements in highly viscous liquid environments, IEEE Sens. J. 5 (2005) 425–432.
- [15] S.J. Martin, G.C. Frye, A.J. Ricco, S.D. Senturia, Effect of surface roughness on the response of thickness-shear mode resonators in liquids, Anal. Chem. 65 (1993) 2910–2922.
- [16] J.D. Larson III, R.C. Ruby, K.L. Telschow, Observation of flexural modes in FBAR resonators at MHz frequencies, in: Presented at Proceedings of the IEEE Ultrasonics Symposium, 2003, October 5–8, 2003, Honolulu, HI, United States, 2003.
- [17] J. Weber, W.M. Albers, J. Tuppurainen, M. Link, R. Gabl, W. Wersing, M. Schreiter, Shear mode FBARs as highly sensitive liquid biosensors, Sens. Actuator. A: Phys. 128 (2006) 84–88.
- [18] IEEE Standard Definitions of Physical Quantities for Fundamental Frequency and Time Metrology—Random Instabilities, IEEE Std 1139–1999, 1999.
- [19] D.S. Ballantine, *Acoustic Wave Sensors: Theory, Design and Physico-chemical Applications*, Academic Press, 1997, 44.

#### Biographies

**Gunilla Wingqvist** is a PhD student at the Solid State Electronics Department, Uppsala university, Sweden, where she has been studying thin film piezoelectric resonator sensors since 2004. In 2003 she received her MSc in Applied Physics and Electrical Engineering at Linköping university, Sweden. Her master thesis project was concerning sputter deposition and characterisation of perovskite ferroelectric thin films and was performed at the thin film division at the Department of Physics and Measurement Technology at Linköping university. Her current research involves development, fabrication and characterisation of the AlN thin film piezoelectric resonator for various sensor applications, mainly biosensors.

**Johan Bjurström** was born 1974 in Timrå, Sweden. He received his MSc in Material Engineering from Uppsala University, Uppsala, Sweden, in January 2002. His thesis work was about Thin Film Bulk Acoustic resonators. He is currently doing his PhD studies in Engineering Science with specialization in Electronics at The Ångström Laboratory, Uppsala University. His research interests include thin film growth of piezoelectric materials, design and modeling of micromachined Film Bulk Acoustic Resonators (FBAR's). His current research focuses on microwave electronics and sensors based on the FBAR technology.

**Lina Liljeholm** received her MSc in Electronics Design Engineering from Linköping University, Sweden, in 2006. Her thesis concerning electroacoustic evaluation of thin film resonators was performed at the Solid State Electronics Department, Uppsala University, Sweden. Here she worked during 2005 and 2006 on a project concerning the fabrication of SMRs as a research engineer and currently is working as a PhD student on the synthesis and characterization of ferroelectric thin films for electroacoustic applications.

**Ventsislav Yantchev** was born in Vratza, Bulgaria, on May 22, 1976. He received his MSc degree in engineering physics and his PhD degree in microwave acoustics from the University of Sofia, Sofia, Bulgaria, in 1999 and 2004, respectively. During 2004–2006 Dr. Yantchev has been a post doctoral research associate at the department of Engineering Sciences at Uppsala University. Currently he is a senior researcher at the same department. Dr. Yantchev's current research interests are towards the design and fabrication of thin film surface, bulk and plate acoustic wave devices. He is also lecturing in graduate and undergraduate courses on microwave electroacoustic devices. URL: <http://hermes.teknikum.uu.se/~veya>.

**Dr. Ilia Katardjiev** is an associate professor at the Angstrom Laboratory, Uppsala University, Sweden. His research interests are in the area of ion-solid interactions, thin film physics, microelectronics as well as electroacoustics.

Among his greatest achievements is the development of the theory of surface evolution as well as the identification of the sputter-yield amplification effect. He is the Director of a number of Swedish and European research programs and leads a group with broad R&D activities in thin film electroacoustic applications, most notably passive and active microelectronic components,

chemical and biochemical sensors, etc. Dr. Katardjiev earned his PhD in Electrical Engineering from Salford University, U.K. in 1989 and since then has been working as a research scientist and a lecturer at Uppsala University. He has published over 100 refereed papers and presented over 20 invited and plenary lectures.